Intercage guest correlations and guest clusters in high-pressure clathrate hydrates

Chris A. Tulk,[1] Dennis D. Klug,[2] Bryan C. Chakoumakos,[1] and Ling Yang[1,3]
[1]*Neutron Scattering Sciences Division, Oak Ridge National Laboratory, Oak Ridge, Tennessee 37831, USA*
[2]*Steacie Institute for Molecular Sciences, National Research Council of Canada, Ottawa Ontario, Canada K1A 0R6*
[3]*Center for Nanophased Materials Sciences, Oak Ridge National Laboratory, Oak Ridge, Tennessee 37831, USA*
(Received 22 April 2009; published 4 August 2009)

The positions of guest atoms in high-pressure hexagonal Kr clathrate hydrate have been determined. Additionally, the large cage guests of the initial cubic form show a displacement of ~0.7 Å from the large cage center and exhibit reduced cage-to-cage correlations in guest positions; similar disorder likely carries over to the high-pressure form. Based on size and electron density maps, up to three atoms are located in the large cage of the high-pressure hexagonal form, where two Kr atoms are 2.25 Å above/below the cage center and one on a ring with a radius 1.70 Å from the cage center.

DOI: 10.1103/PhysRevB.80.052101 PACS number(s): 61.43.−j, 61.05.cp, 62.50.−p

Clathrate hydrates are inclusion compounds where water forms a crystal lattice of cages that contain "guest" molecules or atoms.[1] This system is unique in that it is potentially a source of hydrocarbon fuel as methane hydrate and a storage matrix for man-made greenhouse gases such as carbon dioxide.[2] Its potential as a hydrogen storage medium in the form of a H_2 clathrate form has also been described elsewhere.[3,4] Furthermore, entirely classes of these compounds are being discovered at high-pressure where even the overall crystallographic structures are not well understood.

Three structures have been observed naturally,[5] two cubic structures[6] (sI and sII), and one hexagonal (sH).[7,8] An sH form and other structures have been produced *in situ* at higher pressures with noble gases[9,10] and methane[11] guest species. Each of the cubic structures are made up of small (S) and large (L) water cages denoted as 5^{12} and $5^{12}6^2$ for sI ($S_2 \cdot L_6 \cdot 46\ H_2O$) and 5^{12} and $5^{12}6^4$ for sII ($S_{16} \cdot L_8 \cdot 136\ H_2O$), while the sH form is made up of three types of cages denoted as small, 5^{12}, medium, $4^3 5^6 6^3$, and large, $5^{12}6^8$ ($S_3 \cdot M_2 \cdot L_1 \cdot 34\ H_2O$). The cages are formed by water molecules bonded to form polygons that share edges, e.g., the large $5^{12}6^2$ cage of sI is a tetrakaidecahedron consisting of 12 pentagons and two hexagons.

Molecular dynamics simulations of sII Ar hydrate have produced mean square displacements that indicate large cage guest atoms are rattling substantially and perhaps not located at the cage center.[12] In N_2 clathrate, Rietveld analysis and computer simulation indicate the guest may be off center by almost an angstrom.[13] In the low-pressure methane system, recent attempts using maximum entropy methods (MEM) have resulted in locating methane at the cage center[14] and often the refined structures exhibit very large anisotropic thermal parameters.[15,16] Earlier molecular dynamics simulations of sII Kr hydrate have indicated that the guest might be displaced from the large cage centers.[17] Displacements from the central positions in sI semiconductor clathrates with Si in place of water and hydrogen containing sII clathrate have been identified. In the Si sI clathrate this was suggested to be the result of a strong Jahn-Teller effect.[18] The objective here is to characterize the positional correlations of guests in neighboring cages and the geometry of clusters in large cages of a high-pressure form by combining Rietveld diffraction methods with a direct Fourier transformation analysis.

This study involves high-energy x-ray diffraction from low-pressure sII and high-pressure sH krypton clathrate hydrate samples. This data enables both structure refinement[19] and direct Fourier transformation of the data. The latter analysis provides directly the atom-atom correlations that are not subject to an average crystal model,[20] while the former results in electron density difference maps. Typically in these systems the total x-ray scattering intensity is only weakly weighted to the guest atom correlations. This is due to the high concentration of host atoms and the small difference in the number of electrons between host and guest atoms. However, using heavier guest atoms enhances the relative contribution of the guest to the total scattering intensity. Krypton was chosen because of its simple structure, its higher atomic weight (compared with argon) and because the sH large cages are likely to be multiply occupied.

Kr hydrate samples, sII, were produced at the National Research Council of Canada using a method outlined previously.[21] A subsection of the sample was cold loaded (77 K) into a piston cylinder assembly warmed to 250 K and compressed to 1.8 GPa. There was no indication of transformations of residual ice I, III, or V, providing initial evidence that the samples were pure, this was later confirmed by x-ray diffraction. The sample was then quenched to liquid nitrogen temperature and recovered to atmospheric pressure. Both the quench recovered high-pressure form and the uncompressed sII form were transported to the advanced photon source at liquid nitrogen temperature. X-ray diffraction experiments were performed at sector 11-ID-B, using 0.137024 Å x-rays. Both samples were then loaded into separate sample positions in a He cryostat such that the sample was not raised above 80 K. The sample was heated to 90 K to remove any access liquid nitrogen and then cooled to 40 K. A sample to detector distance of 239.3 mm maximized momentum transfer range for Fourier analysis, $Q_{max}=20$ Å^{-1} and $\Delta d/d = 6\%$ (measured using a CeO_2 crystalline standard), and a detector distance of 700.2 mm provided higher resolution data and $Q_{max}=11$ Å^{-1} and $\Delta d/d=3\%$.

Figure 1 shows the measured diffraction intensity of the data scaled to the weighted atomic form factor. Initial Rietveld refinements using the sII data were made with only the oxygen and krypton atoms included in the model.[22] The initial host atomic coordinates were taken from propane hy-

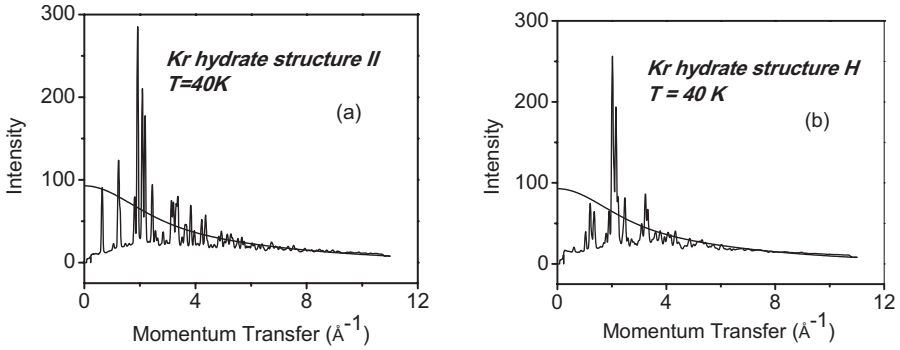

FIG. 1. Total scattering data (higher-resolution setting) collected from the sII and quench recovered sH forms of clathrate hydrate. Data collected at ambient pressure and low temperature for uncompressed sII clathrate hydrate are shown in (a) and data collected from the pressure/temperature quench recovered hexagonal form, sH, are shown in (b). The atomic form factors for the clathrate material are also shown. The *y* axes are plotted in electron units.

drate sII[23] and Kr atoms were positioned at the center of both cage types at (0,0,0) and $(\frac{3}{8},\frac{3}{8},\frac{3}{8})$ for the 5^{12} and $5^{12}6^2$ cages respectively, and their isotropic displacements and site occupancies were allowed to vary. The oxygen atom positions were also allowed to vary along with the isotropic atomic displacement parameters, the lattice parameters, background, two-theta zero, and pseudo-Voigt peak shape parameters.

Figure 2 shows the radial distribution functions generated from direct Fourier transformation of the diffraction data.[24] Simulations of the total radial distribution function[25] based on the fitted model (shown in the lower curves) are used to help interpret the measured g(r) function.[26,27]

The first O-O correlation in Fig. 2(a) appears at a radial distance of 2.78 Å as expected. For the small cage the first Kr-O distance is 3.84 Å, and the large cage Kr-O distance is 4.45 Å. The first intercage Kr-Kr distance is 6.09 Å, consistent with crystallographic small cage data. However, the sII model structure, with the Kr atoms confined to the cage center, generates a g(r) with a strong intercage Kr-Kr peak located at 7.06 Å as indicated with (*) in Fig. 2(a). This correlation is not readily apparent in the measured data and increasing the thermal parameter in the model does not alter significantly the peak width. This discrepancy is also indicated by the Kr-Kr correlations at greater radial distances.

To help reconcile this discrepancy and to establish the details of the cage-to-cage guest correlations for further analysis, the Rietveld data analysis was revisited and a difference Fourier map was calculated from the difference between the measured data and the model data without the Kr atoms, see Fig. 3 where contours are chosen to show features without illustrating weak intensity. Because the Kr atoms contribute a significant fraction of the total electron density (~39%) the difference Fourier map indicates the weighted distribution of electron density from the Kr atoms within the cages.

In the small cages of sII the density maps show that the mean density of the Kr atoms is located at the cage center. However, for the sII large cage, the electron density is located distinctly off center (as suggested in other systems), with a tetrahedral arrangement of positive density at 0.7 Å from the cage center. The off-center krypton density in the Fourier difference map suggested that a fractionally occupied split site might be a better model in the Rietveld refinement. A split-site model with guest atoms located in the 32*e* positions situated along the threefold axes away from the large cage center leads to an improved fit with anisotropic displacement parameters resulting in probability ellipsoids flattened like "pancakes" normal to the threefold axes, thus

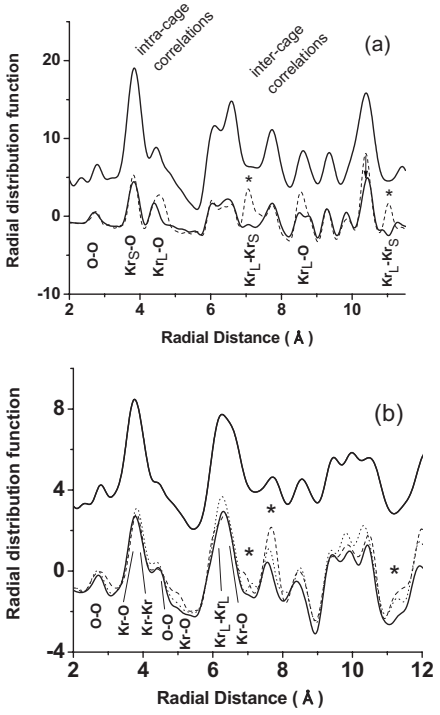

FIG. 2. Calculated and simulated radial distribution functions for two forms of krypton clathrate hydrate. In both plots the dominant atom-atom correlations contributing to each peak are given under the curves. The structure II low pressure from is shown in (a). The upper plot is the experimentally determined data set and the lower plots are the simulated data sets using the cage center model (dashed curve) and the disordered guest site model (heavy curve). The quench recovered high-pressure form is given in (b), with the experimental data in the upper plot and in the lower plot are calculated data from ordered models with two and three guest atoms on the large cage long axis (dotted and dashed respectively) and a disordered model (bold curve) as described in the text.

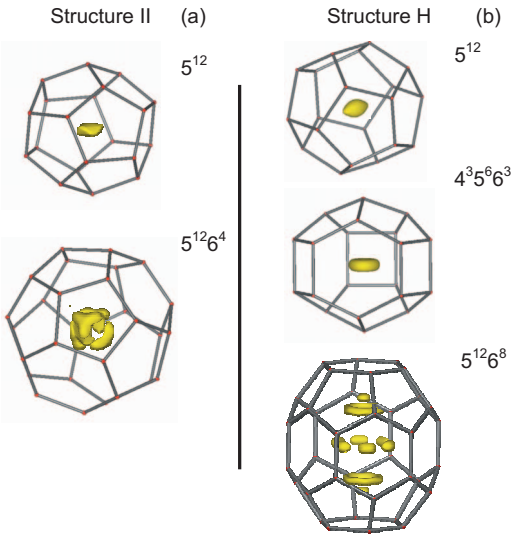

FIG. 3. (Color) This figure presents Fourier difference maps that illustrate the electron distribution of krypton within the water cages. The low-pressure cubic sII form is shown in (a) and the quench recovered high-pressure hexagonal form, sH, is shown in (b). These are given at constant electron density within the cages and at isosurfaces of 1.8 electrons/Å^3 for sII and 2.0 electrons/Å^3 for small and medium cages and 1.2 electrons/Å^3 for the large cage of sH. There appears to be some additional density near the upper and lower rings in sH this is possibly due to the top and bottom atom.

mimicking the electron density in the Fourier difference map. The refined site occupancy of the split site is 0.204(2) compared to the expected 0.25 if there was one krypton atom on average in each large cage. The refined occupation of the small cage is also less than one, 0.877(6). Taken together, the resulting composition, $Kr_{14}\cdot Kr_{6.5}\cdot 136H_2O$ (ideally $(S_{16}\cdot L_8\cdot 136H_2O)$, has 85.4% Kr occupancy. This model displaces the Kr atoms from the cage center opposite a hexagonal polyhedra face. Thus having established the details of the average positional disorder within the large cage a model could be developed to explain the correlations of the pair distribution function and the analysis can be carried onto the high-pressure form.

A second radial distribution function calculation using an sII disordered model based on the split-site analysis above, but with the large cage guest atoms randomly located on these sites between neighboring cages gives a radial distribution function with much weaker correlations between the guest atoms, resulting in the disappearance or at least substantial broadening of the large cage Kr correlations at 7.06 and 11.02 Å. This data is given as the heavy lines in the lower plot of Fig. 2(a). This analysis thus gives reasonable results and provides the basis for analysis below of the high-pressure form.

The large cage, $5^{12}6^8$, in the hexagonal form is roughly "barrel-shaped" with the Fourier difference map showing a ring of Kr density around the girdle and two other krypton sites toward each end of the barrel shown in Fig. 3(b). The small cages have one Kr atom located at the cage centers, $(\frac{1}{2},\frac{1}{2},\frac{1}{2})$ and $(\frac{2}{3},\frac{1}{3},0)$ for the 5^{12} and $4^35^66^3$ cage respectively. For the large cage the ring shown in the figure represents the superposition of atom locations with sixfold symmetry about the long axis of the cage and the cage center at (0,0,0). Given the size of the Kr atoms relative to the cage we expect at most three atoms per cage, one toward each end and one located on the ring around the *waist*. Based on these maps it is possible to identify the size and shape of the Kr clusters in the large cage of a clathrate with full occupancy. The *waist* ring is of ~1.70 Å radius located about the long axis of the cage and at the cage mid height. The two additional rings of Kr density are on the long axis above and below the midplane by ~2.25 Å. Recent molecular dynamics simulations of free energies indicate that Kr occupancies in the large cage could reach three but the free-energy differences between double and triple occupancy are fairly small.[28]

For the sH Rietveld refinement a model was based on the Fourier difference maps and the water to guest ratio was allowed to vary from that determined from the sII refinement, thus it was possible that excess water or Kr could be present in the system in the form of crystalline ice or Kr. As a result the total Kr content for the sH is 5.79 atoms per unit cell (this is close to the Kr content of 5.14 determined in the sII case) gives approximately two Kr atoms *on average* over the entire structure per large cage, with the top and bottom sites located with half occupancy along the cage axis 2.97 Å above and below the cage center, and one site 1/6 occupied located in the equatorial plane surrounding the cage center position (this displacement above and below the cage center is similar to the 2.25 Å found from the difference Fourier maps). However, we emphasize here that for this Rietveld refinement, trying to fit the smeared out electron density with a limited number of spherical or ellipsoidal shaped densities cannot work perfectly and thus the number of krypton atoms per large cage in this Rietveld model is likely too low. The upper plot of Fig. 2(b) shows the measured radial distribution functions of the sH form and the lower plots compare the ordered and disordered models. The calculated radial distribution functions have been determined using a sH structure with one guest Kr atom at the center of the small (5^{12}) and medium ($4^35^{12}6^8$) cages and multiply occupied large cages. The ordered models have either two or three guest atoms located on the sixfold axis of the large cage, these radial distribution functions are given by the dotted and dashed curves respectively. The disordered model has three Kr atoms in the large cage, one at the top and bottom and a third randomly placed on the *ring* to mimic the Fourier difference maps. Some of the atom-atom correlations are given on the figure, but due to the number of correlations it is more difficult to identify specific partials contributing to each of the peaks beyond 6.5 Å, however, the three peaks between 8.5 and 11 Å are due to correlations involving Kr-Kr and Kr-O correlations, with the two greater distance peaks in this range being predominantly from Kr-Kr correlations. The calculated pair distribution functions of the ordered models indicate increasing intensity with two or three guests, particularly at radial distances between 6.5 and 8.5 Å, this is not consistent with the measured data. It is clear that such as the sII case, the ordered sH models tested here are not good representations of the guest disorder in the sH large cage.

This total scattering analysis appears to give little correlation in the position or relative orientation of Kr clusters between neighboring *large* cages at 40 K. The radial distribution functions are well described when the guest atoms in the large cages are placed randomly based on locations of greater density in the Fourier difference map. While the correlations between atoms in small cages is well defined, this analysis indicates that the interaction distance with guest atoms in large cages may not extend beyond the immediate cage environment, thus lending support to previously formulated models of thermal conductivity.[29]

Oak Ridge National Laboratory is supported by the Division of Materials Sciences, U.S. D.O.E. (Contract No. DE-AC05-00OR22725 with UT-Battelle, LLC). The authors would like to thank J. M. Simonson, J. Horita, and D. Cole for providing laboratory space in the Chemical Sciences Division at Oak Ridge National Laboratory.

[1] G. W. Jeffrey and R. K. McMullan, in *Progr. Inor. Chem*, edited by F. A. Cotton (John Wiley and Sons, New York, London, Sydney, 1967), p. 43.
[2] E. D. Sloan, *Clathrate hydrates of natural gasses*, 2nd ed. (Dekker, New York, 1998).
[3] W. L. Mao *et al.*, Science **297**, 2247 (2002).
[4] K. A. Lokshin, Y. Zhao, D. He, W. L. Mao, H. K. Mao, R. J. Hemley, M. V. Lobanov, and M. Greenblatt, Phys. Rev. Lett. **93**, 125503 (2004).
[5] H. Lu *et al.*, Nature (London) **445**, 303 (2007).
[6] G. A. Jeffrey, in *Inclusion Compounds*, edited by J. L. Atwood, J. E. D. Davies, and D. D. MacNicol (Academic, London, 1984), Vol. 1, p. 135.
[7] J. A. Ripmeester, J. S. Tse, C. I. Ratcliffe, and B. M. Powel, Nature (London) **325**, 135 (1987).
[8] K. A. Udachin, C. I. Ratcliffe, and J. A. Ripmeester, Supramol. Chem. **2**, 405 (2002).
[9] A. G. Ogienko *et al.*, J. Phys. Chem. B **110**, 2840 (2006).
[10] A. Y. Manakov *et al.*, J. Inclusion Phenom. Macrocyclic Chem. **48**, 11 (2004).
[11] J. S. Loveday *et al.*, Nature (London) **410**, 661 (2001).
[12] H. Itoh, J. S. Tse, and K. Kawamura, J. Chem. Phys. **115**, 9414 (2001).
[13] W. F. Kuhs, B. Chazallon, P. G. Radaelli, and F. Pauer, J. Inclusion Phenom. Macrocyclic Chem. **29**, 65 (1997).
[14] A. Hoshikawa, N. Igawa, H. Yamauchi, and Y. Ishii, J. Chem. Phys. **125**, 034505 (2006).
[15] J. Baumert, C. Gutt, M. R. Johnson, J. S. Tse, D. D. Klug, and W. Press, J. Chem. Phys. **120**, 10163 (2004).
[16] C. Gutt, *et al.*, J. Chem. Phys. **113**, 4713 (2000).
[17] J. S. Tse and M. L. Klein, J. Phys. Chem. **91**, 5789 (1987).
[18] F. Brunet, P. Mélinon, A. San Miguel, P. Kéghélian, A. Perez, A. M. Flank, E. Reny, C. Cros, and M. Pouchard, Phys. Rev. B **61**, 16550 (2000).
[19] A. C. Larson and R. B. Von Dreele, Los Alamos National Laboratory Report No. LAUR 86-748, 2000 (unpublished); B. H. Toby, J. Appl. Crystallogr. **34**, 210 (2001).
[20] T. Egami, *Underneath the Bragg Peaks: Structural Analysis of Complex Materials. pergamon materials series* (Pergamon, Amsterdam, Boston, 2003), Vol. 7.
[21] Y. P. Handa, J. Chem. Thermodyn. **18**, 891 (1986).
[22] The 272 H atoms in the unit cell only contribute 12.2% of the electron density, and thus they were not included.
[23] C. J. Rawn, Can. J. Phys. **81**, 431 (2003).
[24] X. Qiu, J. W. Thomson, and S. J. L. Billinge, J. Appl. Crystallogr. **37**, 678 (2004).
[25] Th. Proffen and R. B. Neder, J. Appl. Crystallogr. **30**, 171 (1997).
[26] Y. S. Badyal *et al.*, J. Chem. Phys. **112**, 9206 (2000).
[27] Data used for Fourier analysis were corrected for a measured empty sample can, cryostat, and Compton scattering and was then scaled to the atomic form factor for the sample. A standard empirical data correction was applied to remove a slope that originated from the detector edge effects (see 26). The Fourier transform used a Qmax of 20 $Å^{-1}$. The simulations employed a host lattice of water molecules from the reitveld refinements and guest atoms (192 for sII and 64 for sH) filling cages as discussed in the text.
[28] S. Alavi, J. A. Ripmeester, and D. D. Klug, J. Chem. Phys. **125**, 104501 (2006).
[29] J. S. Tse *et al.*, Nature Mater **4**, 917 (2005).